

Supporting information

Magnetic and near-infrared-II Fluorescence Au-Gd Nanoclusters for Imaging-Guided Sensitization of Tumor Radiotherapy

*Hui Zhao^{a, 1}, Hao Wang^{b, 1}, Hairu Li^c, Tiecheng Zhang^a, Jing Zhang^a, Wenhui Guo^a, Kuang Fu^{a, *}, Guoqing Du^{c, d, *}*

^a Department of MRI Diagnosis, The Second Affiliated Hospital of Harbin Medical University, Harbin 150086, Heilongjiang Province, P. R. China

^b Department of Respiratory and Critical Care Medicine, The Second Affiliated Hospital of Harbin Medical University, Harbin 150086, Heilongjiang Province, P. R. China

^c Department of Ultrasound, The Second Affiliated Hospital of Harbin Medical University, Harbin 150086, Heilongjiang Province, P. R. China

^d Department of Ultrasound, Guangdong Provincial People's Hospital, Guangdong Academy of Medical Sciences, Guangzhou 510080, Guangdong Province, P. R. China

¹ Hui Zhao and Hao Wang contributed equally to this work.

* Corresponding authors. E-mail: duguoqing@hrbmu.edu.cn (Guoqing Du), 3996@hrbmu.edu.cn (Kuang Fu).

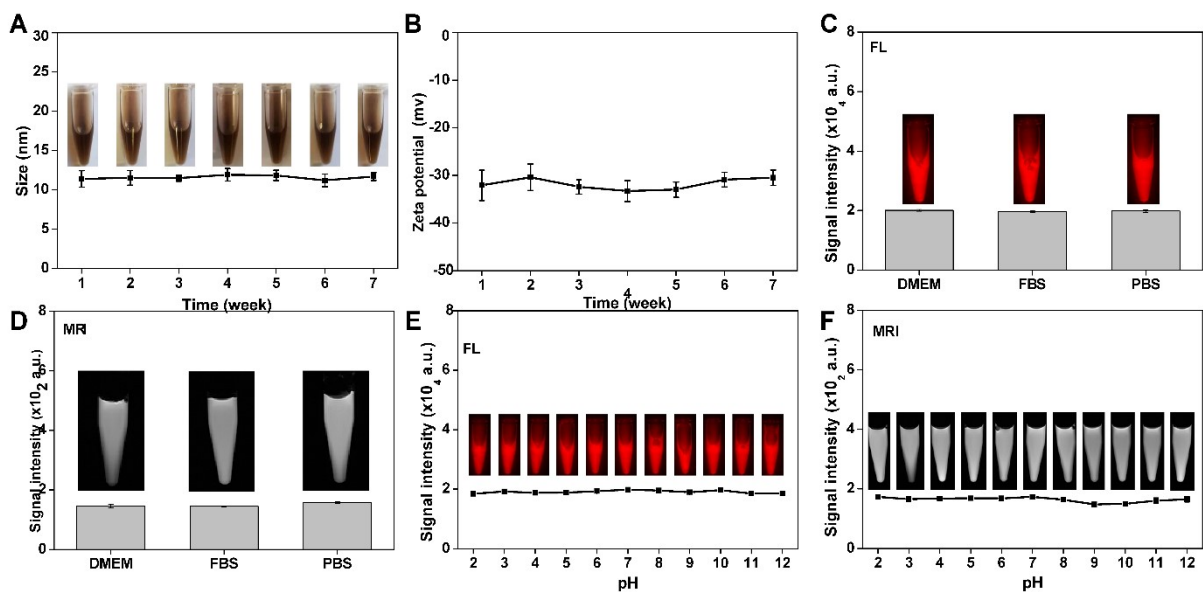


Figure S1. Characterization of Au-Gd NCs. **A)** The hydrodynamic diameter variation of Au-Gd NCs in 7 weeks. The insets: digital photograph of Au-Gd NCs in 1st to 7th week after synthesis. **B)** The zeta potential variation of Au-Gd NCs in 7 weeks. **C)** The NIR-II FL intensity of Au-Gd NCs with the same concentration in DMEM, FBS and PBS (pH 7.4, 0.1 M) solution. The insets: NIRF-II images of Au-Gd NCs in different solutions. **D)** The MRI signal intensity of Au-Gd NCs with the same concentration in DMEM, FBS and PBS (pH 7.4, 0.1 M) solution. The insets: MRI images of Au-Gd NCs in different solutions. **E)** The NIR-II FL intensity of Au-Gd NCs with the same concentration in solution with different values of pH (2-12). The insets: NIRF-II images of Au-Gd NCs with different pH values. **F)** The MRI signal intensity of Au-Gd NCs with the same concentration in solution with different values of pH (2-12). The insets: MRI images of Au-Gd NCs with different pH values

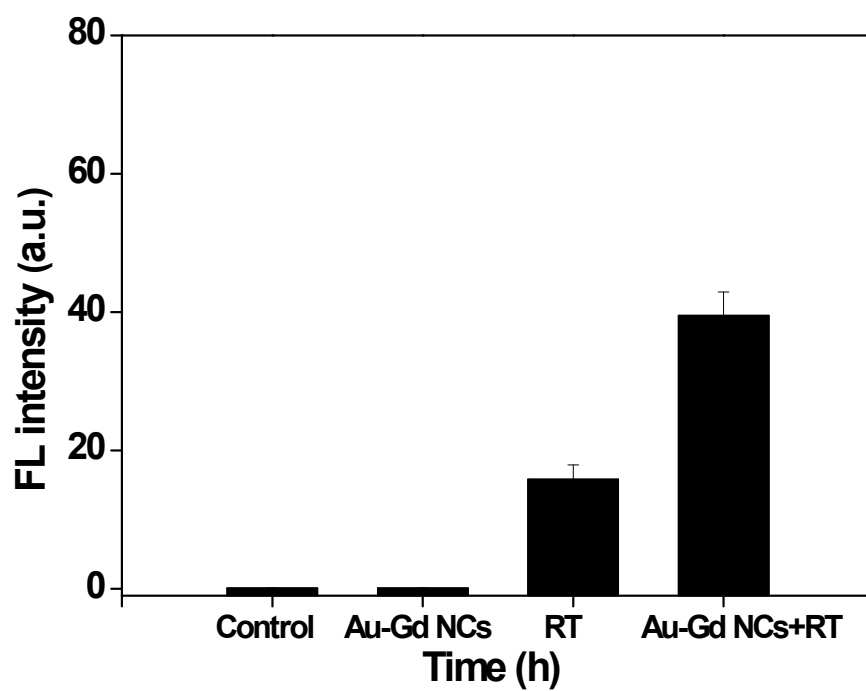


Figure S2 Semiquantification of γ -H₂AX density using the Image J software.

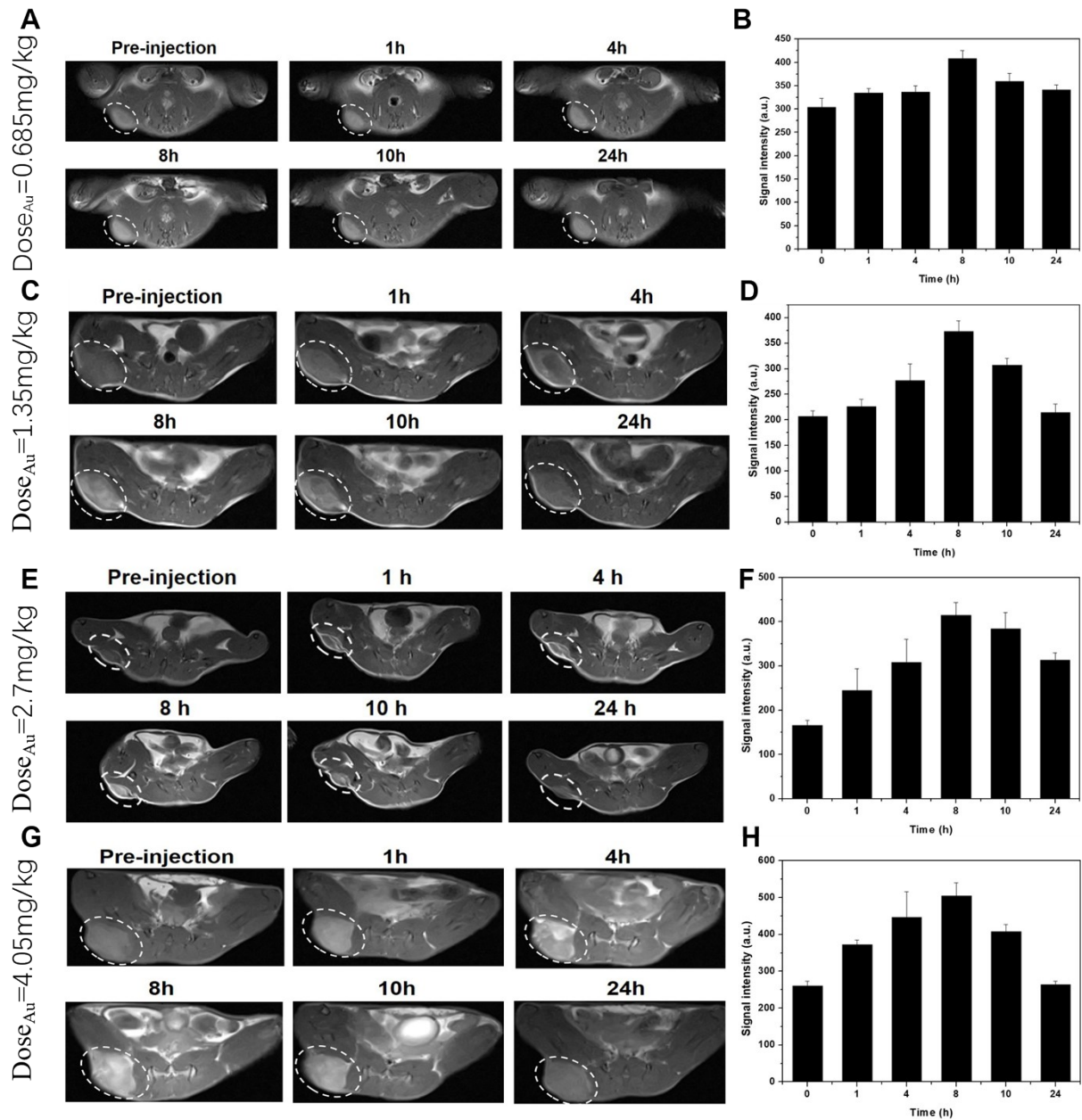


Figure S3 In vivo MR imaging of tumors. A,C,E,G) T1-weight MRI images of Au-Gd NCs in C6 subcutaneous tumor-bearing mice at different time intervals. B,D,F,H) Quantitative analysis of tumor signal intensity at different time points after IV injection of Au-Gd NCs.

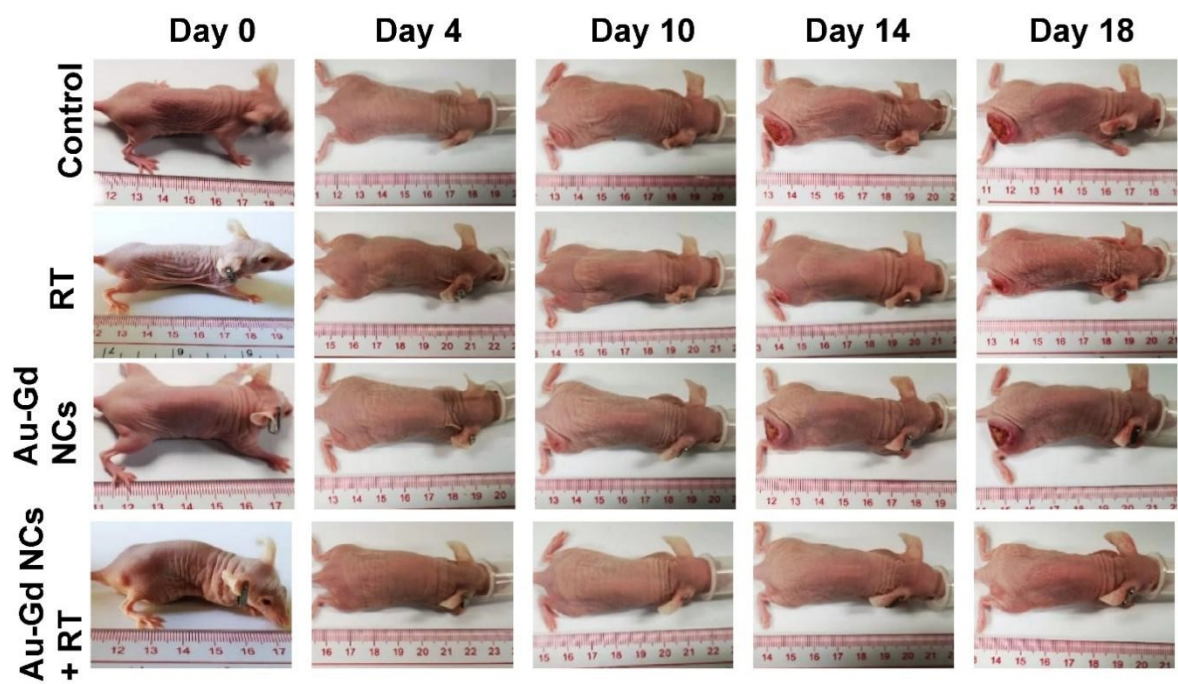


Figure S4. Photographs of mice with different treated groups.

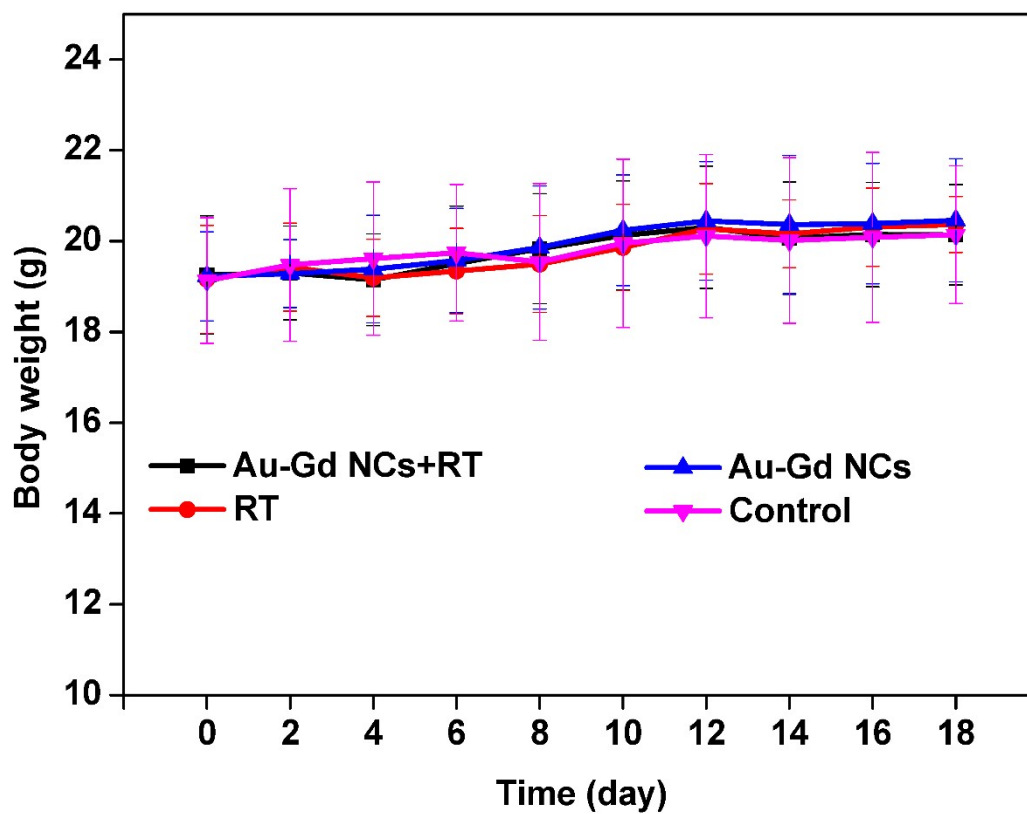


Figure S5. Body weights of tumor-bearing nude mice with different treatments during the 18 day evaluation period.